

Dynamics of neutralizing electrons and the focusability of intense ion beams in HIF accelerating structures

A.F. Lifschitz^a, G. Maynard^a, J.-L. Vay^b

^aLaboratoire de Physique des Gas et des Plasmas, CNRS-UMR8578, Université Paris XI, Orsay, France

^bLawrence Berkeley National Laboratory, 1 Cyclotron Road Bldg 47/112, Berkeley, CA 94720, USA

Abstract

In most of the proposals for HIF reactors, beams propagate ballistically through the containment chamber. To get the required final radius (~ 3 mm), the charge of the beam must be neutralized to some extent. Several neutralization schemes are possible, as co-injection of negative-ions beams, inclusion of external sources of electrons, or it can be provided by electrons coming from ionization of the background gas. In this work, we study the role of the electron dynamic on the neutralization and final radius of the beam. This is done by performing fully-electromagnetic PIC simulations of the beam ballistic transport using the BPIC code[1]. In agreement with previous works we found that the evolution of an isolated beam is well described as a bidimensional adiabatic compression, and the beam neutralization degree and final radius can be estimated from the initial electron transversal temperature. When a background gas is present the evolution differs significantly from an adiabatic compression. Even for low gas densities, the continuous electrons flow coming from gas ionization limits efficiently the compressional heating, thus reducing the final radius. Aspects of beam neutralization by background gas ionization are discussed.

1. Introduction

A key issue in HIF is to deposit a significant part of the energy carried by the beams over the small surface of the target. Two modes for transporting the beam across the confinement chamber have been considered, channel-like-transport and ballistic transport [1]. In the first mode, an azimuthal magnetic field, created by the beam or preformed in some way, balances the radial expansion caused by the beam own space charge. In the second approach, the beams are focalized before entering the

chamber and travel ballistically to the target, a distance of $\simeq 3$ m. For the currents needed in a reactor, the beam space charge must be neutralized in order to get the required final radius. The problem of the beam neutralization have been the object of several studies, including analytical and semi-empirical works [2,3] and PIC simulations [4–6]. In this work we study the role of the electron dynamic in the screening of the beam and its propagation and final radius using a fully-electromagnetic 2 $\frac{1}{2}$ -dimensions (r, z) PIC code [7]. In section 2 we study the case of neutralized beams isolated from any source of electrons. Beam interacting with the plasma created by ionization of the background gas that fills the chamber are considered in section 3.

Email address: agustin.lifschitz@lpgp.u-psud.fr
(A.F. Lifschitz).

2. Electrons temperature and neutralization of an isolated beam

Even when the system is globally neutral, i.e. the total electron charge equals the total beam charge, the degree of neutralization is not perfect because of the finite transversal electronic temperature. For beams with radius much smaller than axial length $r_b \ll L_b$, the degree of neutralization depends on the ratio between the beam radius and the Debye length and on the shape of the radial density profile. Numerically solving the Poisson-Boltzmann equation for an infinite cylindrical beam in equilibrium, we obtained the following fitted expressions for the neutralization degree,

$$f_{\text{flat}}(\chi) = 1 - 3/(\chi + 0.7)^{1.16} \quad \text{flat profile} \quad (1)$$

$$f_{\text{gauss}}(\chi) = 1 - 30/(\chi + 3)^{2.2} \quad \text{gaussian profile} \quad (2)$$

with

$$\chi = \frac{\hat{r}_b}{\hat{\lambda}_D} = \sqrt{\frac{e^2 Z N_b}{\epsilon_0 \pi \hat{L}_b k \hat{T}_{e\perp}}}, \quad (3)$$

$$\hat{\lambda}_D = \sqrt{\frac{\epsilon_0 k \hat{T}_{e\perp}}{e^2 n_0}}, \quad n_0 = \frac{Z N_b}{\pi \hat{r}_b^2 \hat{L}_b},$$

where \hat{r}_b is the rms radius defined by $\hat{r}_b = \sqrt{2\langle r^2 \rangle}$, \hat{L}_b is the rms beam length, N_b is the number of beam ions and Z the ion charge in units of the electron charge. The rms transversal electron temperature is defined as $\hat{T}_{e\perp} = \langle \hat{T}_{ex} \rangle + \langle \hat{T}_{ey} \rangle$. Brackets denote average over the cross section, $\langle X \rangle = \int 2\pi r dr X(r)n(r) / \int 2\pi r dr n(r)$. For a flat profile \hat{r}_b is the beam radius and $\hat{\lambda}_D$ is the usual Debye length of an homogeneous plasma. The fittings are valid in the range $2.5 < \chi < 50$ with an error $< 5\%$.

Assuming that the beam is isolated from any source of electrons, which implies to neglect ionization of the background gas and ionization of the beam ions, the system evolves isentropically. As the beam approach to the focal point, the electrons are compressed and their temperature raises. If the electrons behave as a bidimensional gas, the following expression for the temperature as a function of a characteristic radius of the volume occupied by the electron cloud can be derived [2]

$$\hat{T}_e = \hat{T}_{e0} \left(\frac{r_{e0}}{r_e} \right)^2. \quad (4)$$

For a tridimensional adiabatic compression/expansion the corresponding expression is

$$\hat{T}_e = \hat{T}_{e0} \left(\frac{r_{e0}}{r_e} \right)^{4/3}. \quad (5)$$

Figure 1 shows the evolution of the transversal electron temperature for a system with global neutrality calculated with the PIC code [a 2 1/2-dimensions (r, z) PIC simulation], rms quantities are averaged over the beam length. The beam is composed by 2.5 GeV-Xe⁺ with average current $I_b = 2.5$ kA, initial radius $\hat{r}_0 = 0.05$ m, length $L_b = 0.5$ m (pulse length 8 ns), unnormalized emittance $\epsilon = 0.05$ mm rad and focal length $L_f = 3$ m. Both the radial and longitudinal initial density profiles are flat. The beam midplane reaches the focal point at $t \approx 52$ ns and the final radius is 0.003 m. The transversal temperature grows from the initial value (0.8 keV) to 60 keV at the point of maximum compression. The bidimensional and tridimensional adiabatic evolution calculated with equations 4 and 5 with the rough approximation $r_e = \hat{r}_b$ are also shown. The bidimensional case is close to the simulation result up to ≈ 15 ns. At this time the beam radius ($\hat{r}_b \approx 0.03$ m) is still much larger than the Debye length $\hat{\lambda}_D \approx 0.001$ m. As the beam radius diminishes, the approximation $r_e = \hat{r}_b$ becomes worse and the bidimensional results duplicates the PIC value around the focal point. The value $r_e = \sqrt{\hat{r}_b^2 + 4\hat{\lambda}_{D0}^2}$ used in ref. [2] also results in this case in a overestimation of the temperature, by a factor $\simeq 1.8$ at the focal point. This lack of agreement between the temperature corresponding to a bidimensional compression and the numerical result is due to an inadequate estimation of the volume of the electron cloud. As can be seen in figure 2, a better agreement is obtained using $r_e = \hat{r}_e$, with \hat{r}_e the rms electron radius obtained from the PIC simulation. This form for r_e cannot be included in an scheme based in the envelope equation formalism, because \hat{r}_e is *a priori* unknown. Simulation results show that a good choice for the radius of the electron cloud is

$$r_e = \hat{r}_b + \kappa \hat{\lambda}_{D0} \quad \text{with } \kappa \simeq 3. \quad (6)$$

The three dimensional nature of the process becomes apparent when the beam approaches the focal point and large density gradients between the head and tail occur. Figure 3 shows the spatial distribution of electronic and ionic density for three times, 50 ns, 53 ns and 56 ns. Local temperature is indicated with gray levels. At $t = 50$ ns the head of the beam reaches the focal point. The temperature in the region of maximum compression is higher for both electrons and ions, with maxima of ≈ 120 keV and ≈ 400 keV respectively. At $t = 53$ ns and $t = 56$ ns the position of the peak temperature of ions also corresponds to the instantaneous position of the maximum compression point, reflecting the fact that beam ions behave as a bidimensional system. This is not the case of the electrons. The peak of electronic temperature, that at $t = 50$ ns was at the beam head, smooths quickly and for later times the electronic temperature becomes uncorrelated with the density and with the ionic temperature. The process involves a displacement of electrons from the high density region toward the less compressed regions and a transfer of energy from the transversal to the longitudinal direction, visible in the rapid increment of \hat{T}_{ez} for $t > 45$ ns (figure 2).

To calculate the neutralization degree we assume that the process is a bidimensional isentropic compression given by equations 4 and 6, thus obtaining for the parameter χ (equation 3):

$$\chi = \frac{\hat{r}_b + 3\hat{\lambda}_{D0}}{\hat{\lambda}_{D0}}. \quad (7)$$

Figure 4 shows the neutralization degree as a function of time for the same beam parameters for three initial density profiles, (a) a gaussian radial profile/flat longitudinal profile, (b) a gaussian/gaussian profile and (c) a flat/flat profile. For the beam with gaussian radial profile and flat longitudinal profile (4.a), the function f_{gauss} gives a good approximation of the numerical simulation. As can be expected, for the beam with non-uniform axial profile the agreement is not so good, the minimum value given by f_{gauss} is slightly lower than the PIC result (4.b). In the case of a flat radial profile (4.a) the function f_{flat} approximates well the PIC curve for $t < 20$ ns, but it predicts a too low neutralization degree for later times. The

reason is the progressive smoothing of the initial step profile to a gaussian-like profile, visible in the simulations. As can be seen in figure 4.c, f_{gauss} is close to the PIC curve for $t > 40$ ns, giving a good value for the minimum of the neutralization degree at the focal point.

3. Neutralization by ionization of background gas

Electrons coming from ionization of the background gas can contribute to the neutralization of the beam. For heavy ions ($A > 200$) and high gas densities ($n_g \approx 5 \times 10^{19} \text{ m}^{-3}$) it has been shown that these electrons can provide enough neutralization to get the required final radius without any additional electron source [5,4]. For lighter ions as Xe, and lower gas densities ($n_g \approx 7 \times 10^{18} \text{ m}^{-3}$) additional mechanism are needed [8]. The neutralization degree is determined by the gas ionization rate, the time taken by gas ions to leave the beam and the fraction of electrons picked-up by the beam. The number of electrons n_e as a function of the time is given by

$$n_e = N_b \sigma_g n_g v_b t. \quad (8)$$

Following [5], the change in the number of gas ions inside the beam (n_i) is calculated as the difference between ions created and axial losses through the following equation

$$\frac{dn_i}{dt} = N_b n_g \sigma_g v_b - \left(1 + \text{Min} \left(\frac{v_b t}{L_b}, 1 \right) \right) n_i.$$

The solution can be written as a combination of exponentials and the error function. A good approximation to the solution is given by

$$n_i = \frac{1}{2} \sigma_g n_g N_b L_b \left(1 - e^{-(1+v_b t/L_b)^2 + 1} \right). \quad (9)$$

Combining equations 8 and 9 and assuming that all the electrons are picked-up by the beam, we obtain the following expression for the neutralization degree

$$f_1 = \sigma_g n_g \left[v_b t - \frac{1}{2} L_b \left(1 - e^{-(1+v_b t/L_b)^2 + 1} \right) \right]. \quad (10)$$

As the beam becomes neutralized, the assumption of complete picking-up is not longer valid. Numerical simulations show that equation 10 is valid for $t/\sigma n_g v_b \ll 1$. The maximum neutralization degree by axial electron pick-up from a plasma depends on the ratio between the initial kinetic energy of the electrons in the beam frame system and the magnitude of the electrostatic potential well created by the beam charge. For a plasma with a number of electrons $\gg N_b$ or in contact with a source of electrons the limit is given by [1,3]

$$f_e = \left(1 - \alpha \frac{2\pi\epsilon_0 m_e v_b^2 \hat{L}_b}{Z_b e^2 N_b} \right), \quad (11)$$

where α is a number between 1 and 4, Z_b is the beam ion charge number, m_e and e the electron mass and charge respectively. In the case of the plasma created by gas ionization there is a competition between the beam and the plasma for picking-up the electrons. In analogy with the derivation of equation 11 [3], we can obtain an rough indication of the maximum neutralization degree from the following equation

$$\alpha \frac{m_e v_b^2}{2} = \Delta\phi_b - \Delta\phi_g \quad (12)$$

with

$$\Delta\phi_b = \frac{e}{4\pi\epsilon_0} \frac{Z_b N_b - \gamma N_g}{L_b}, \quad \Delta\phi_g = \frac{e}{4\pi\epsilon_0} \frac{\gamma N_g}{L_g}.$$

The LHS of equation 12 is the electron kinetic energy in the beam frame system, and the RHS is the difference between the depth of the electrostatic potential wells created by the beam and the plasma. Assuming $L_g = v_b t$, the neutralization degree can be written as

$$f_2 = f_e \frac{v_b t}{v_b t + L_b}. \quad (13)$$

f_2 is equal to f_e multiplied by a time-dependent factor involving the beam length size and velocity. For $t \rightarrow \infty$, $f_2 \rightarrow f_e$. The dependence with the beam current introduced by f_e is weak. For HIF parameters $f_e > 0.9$. For simplicity we will take $f_e = 1$ in following figures, thus f_2 will be independent of I_b . Better estimations to be published elsewhere also indicate that the values of L_b and L_g mainly determine the long term neutralization.

For the PIC simulations we assume that the background gas is FLIBE. Collision processes included are single ionization of the beam ions by collision with the gas atoms, single ionization of the gas atoms by collision with beam ions and with electrons. Cross sections for this processes are calculated using first-order perturbation theory with an OPAL effective potential [9]. Figure 5 shows the neutralization degree for selected values of I_b and n_g and two beam lengths, $L_b = 0.3$ m (5.a) and $L_b = 0.6$ m (5.b). Stripping of beam ions is not included in this figure, i.e. the beam charge state is frozen. For early times the neutralization is better for the highest density, and it is close to the value predicted by equation 10. As equation 13 predicts, the dependence with the beam current is very weak and the difference between the curves corresponding to same L_b but different n_g becomes small for large times. On the other hand, the quantitative agreement is not very good, the value of f_2 is too large compared with the numerical result. The result of the competition for picking-up electrons is that, for long term, the neutralization does not grow with the gas density. The larger number of electrons created for larger n_g (or larger σ_g) is compensated by the larger number of gas ions in the plasma at the beam tail. The overall behaviour is similar when beam ionization is included, although the dynamic is more complex due to the growth of the gas ionization cross section with the beam charge number and the stripping of beam ions, that will *a priori* reduce the neutralization degree. More work is required to clarify the subject.

The neutralization plays a major role in the determination of the transversal electron temperature. The first electrons created are accelerated by the electrostatic field of the fully-unneutral initial beam, reaching a transversal temperature T_0 that depends on the beam space charge and its shape, typically of some tens of keV. As the neutralization degree grows, the new electrons created see a weaker electric field and reach temperatures $< T_0$, therefore the total electron temperature decreases. The electron cooling caused by this flow of electrons into the system overcomes the compressional heating for a significant part of the beam propagation to the target. Assuming that electrons injected at a given time t reach a temperature $T_0 e^{-t/\tau_1}$ in a

time τ_2 , with $\tau_1 = (\sigma_g n_g v_b)^{-1}$ a characteristic neutralization time, the following expression for the transversal electron temperature can be obtained

$$T_c = \frac{T_0 \tau_1}{t(\tau_1 - \tau_2)} \left[(1 - e^{-\frac{t}{\tau_1}}) \tau_1 - (1 - e^{-\frac{t}{\tau_2}}) \tau_2 \right]. \quad (14)$$

We set τ_2 to the time taken by the initial beam potential to accelerate an electron from the axis to \hat{r}_b . Figure 6 shows the evolution of the transversal electron temperature. Two curves are displayed, one corresponds to the transversal temperature of the electrons inside the beam and the second one corresponds to the electrons in the plasma tail behind the beam. The temperature of the electrons in the plasma is larger than the beam electrons temperature for $t < 40$ ns, the most energetic electrons are more likely to escape from the beam. Compressional heating overcomes the flow-cooling only when the beam is close to the focal point ($t \approx 40$ ns), and the temperature of electrons in the beam region start to grow. Heat transfer from the beam to the tail causes an increment of the plasma temperature, that departs for $t > 47$ ns from the estimation given by T_c that only includes flow-cooling. The role of the heat transfer from the beam to the tail and the cooling of the beam in this last etage must be studied more detaily.

4. Conclusions

Numerical simulations of the ballistic beam propagation show that the approximation of considering the process as an bidimensional adiabatic compression is adequate when the beam is isolated from any source of electrons. The application of this approximation to calculations based in the envelope equation requires some care in the selection of the volume of the electron cloud, that determines the temperature and the bean evolution. Transfer of radial energy to the axial direction takes place when large density and temperature gradients occurs close to the focal point.

The electron flow into the beam originated in ionization of the background gas reduce drastically the effect of the beam compression. The transversal electron temperature reaches high values (≈ 50

keV for $I_b=3$ kA) when the beam enters to the chamber, due to the acceleration of the electrons by the unneutralized beam space charge. The neutralization of the beam reduces the final energy of the new electrons, thus reducing the temperature. If the final radius is of some mm, beam compression heating takes place close to the focal point.

Finally, the growing of the neutralization degree with the density of the background gas is visibly reduced by the capture of a fraction of the electrons by the plasma created by the gas ionization. For large times, the neutralization shows little variation with the gas density. The contact of this plasma with an external conductor or a plasma at the chamber entrance can modify the situation, allowing the flow of more electrons to the system beam + ionized-gas, thus improving the neutralization.

References

- [1] C.L. Olson, Nucl. Instr. and Meth. A, 464 (2001) 118.
- [2] D.S. Lemons, M.E. Jones, Proceedings of the HIF conference, Washington, 1986, p. 287.
- [3] C.L. Olson, Proceedings of the HIF conference, Washington, 1986, p. 215.
- [4] D.A. Callahan, Fusion Eng. and Design, 32-33 (1996) 441.
- [5] J.-L. Vay, C. Deutsch, *Current Trends in International Fusion Research-Proceedings of the Third Symposium*, edited by E. Panarella, Canada, 2002.
- [6] W.M. Sharp, D.A. Callahan-Miller, A.B. Langdon, M.S. Armel, J.-L. Vay, Nucl. Instr. and Meth. A, 464 (2001) 284.
- [7] J.-L. Vay, C. Deutsch, Fus. Eng. Des. 32-33 (1996) 467.
- [8] W.M. Sharp *et al*, 2nd IAEA Technical Meeting on Physics and Technology of Inertial Fusion Energy Targets and Chambers, San Diego, California, 2002.
- [9] S. Mabong, Ph. D. Thesis, Université Paris XI, 1996.

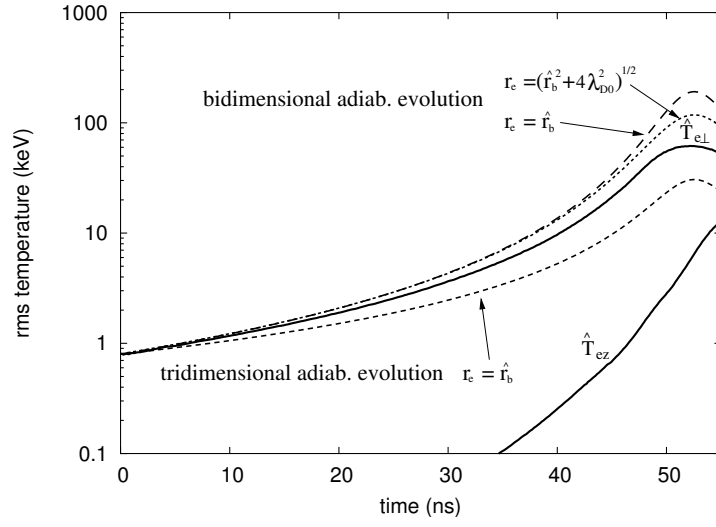


Fig. 1. Evolution of the transversal and axial electron temperature. Initial transversal electron temperature is 0.8 keV.

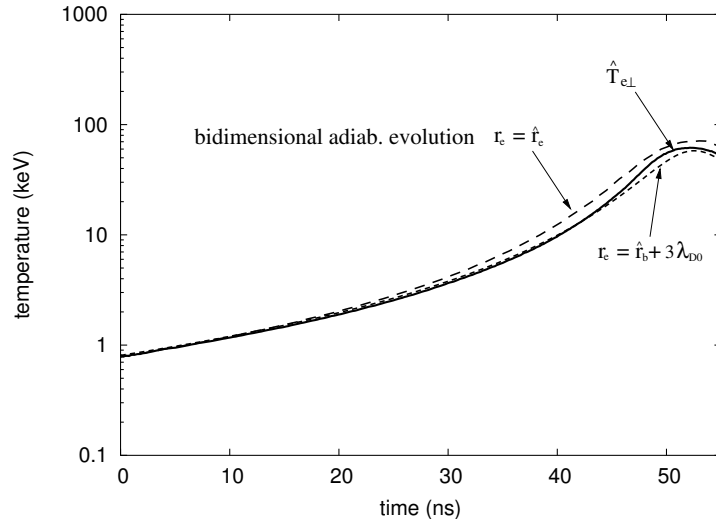


Fig. 2. Evolution of the transversal plasma temperature and the bidimensional adiabatic prediction for two possible choices for r_e .

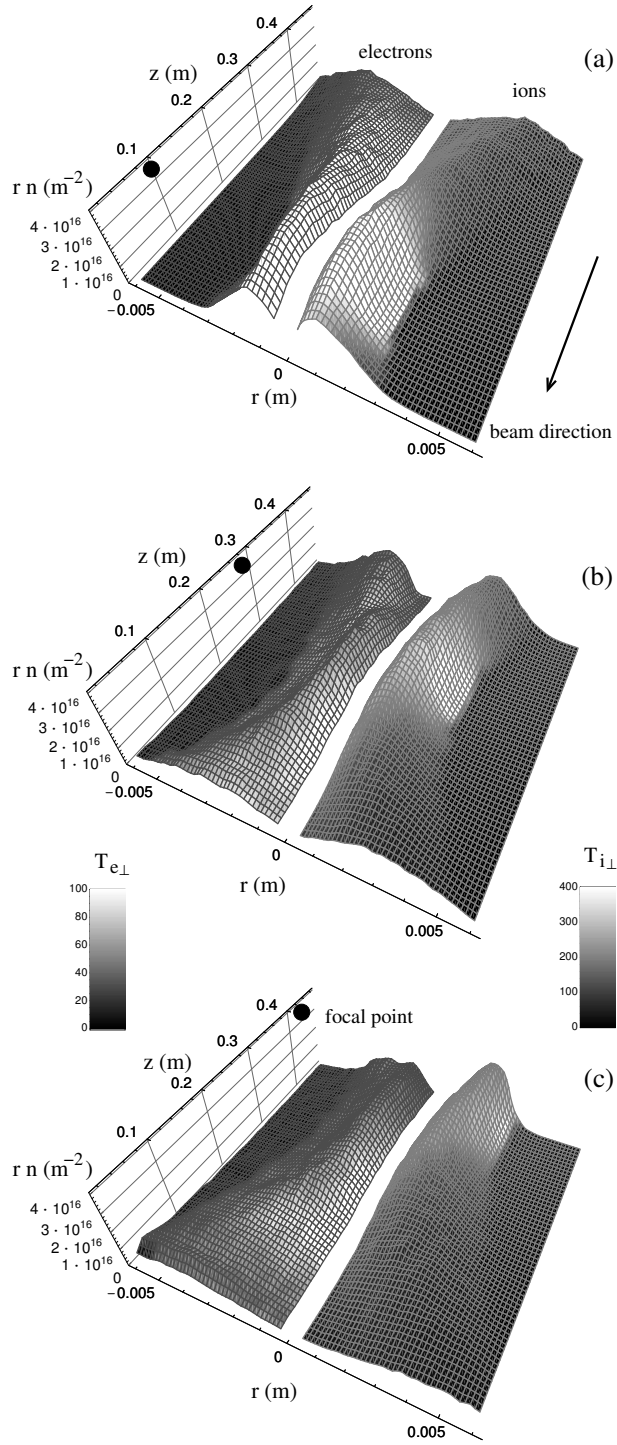


Fig. 3. Spatial distribution of electron density (left part of the plots) and ionic density (right) at time (a) 50 ns, (b) 53 ns and (c) 56 ns. Gray levels indicate local transversal temperature.

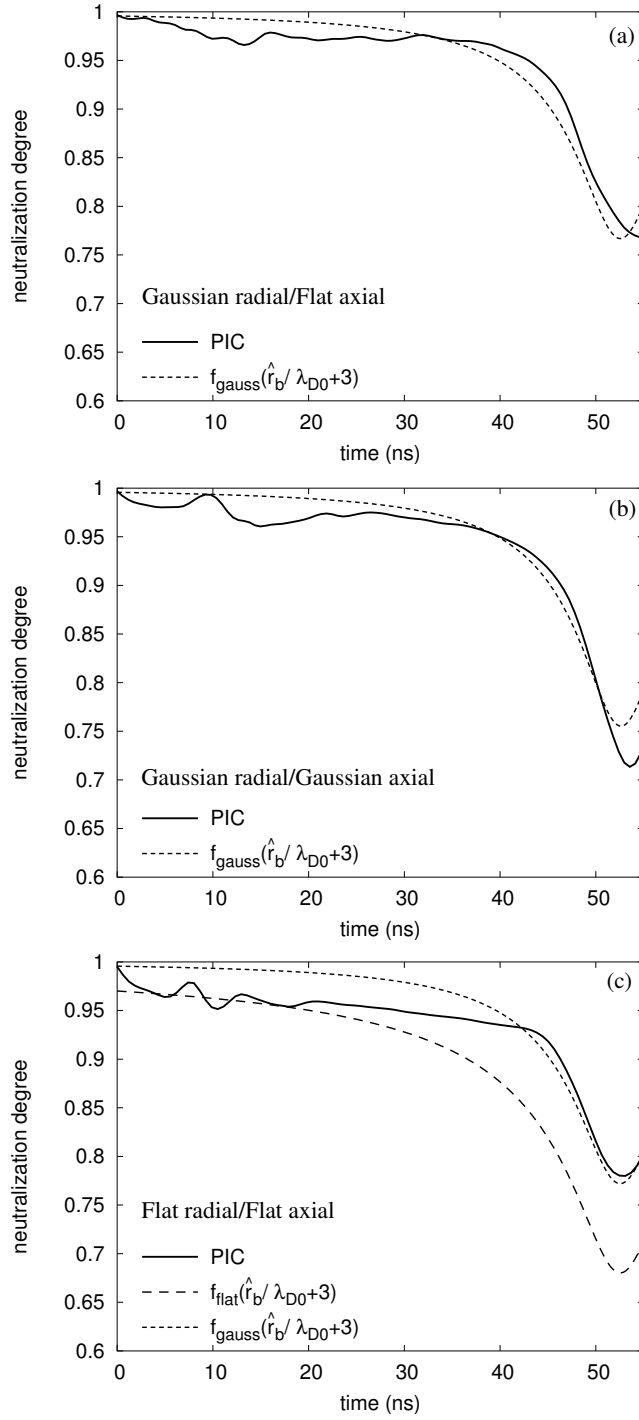


Fig. 4. Neutralization degree of an initially neutral beam as a function of time for selected beam profiles. (a) a beam with gaussian radial profile and flat axial profile, (b) gaussian radial and axial profiles and (c) flat radial and axial profiles. Initial electron transversal temperature 0.8 keV.

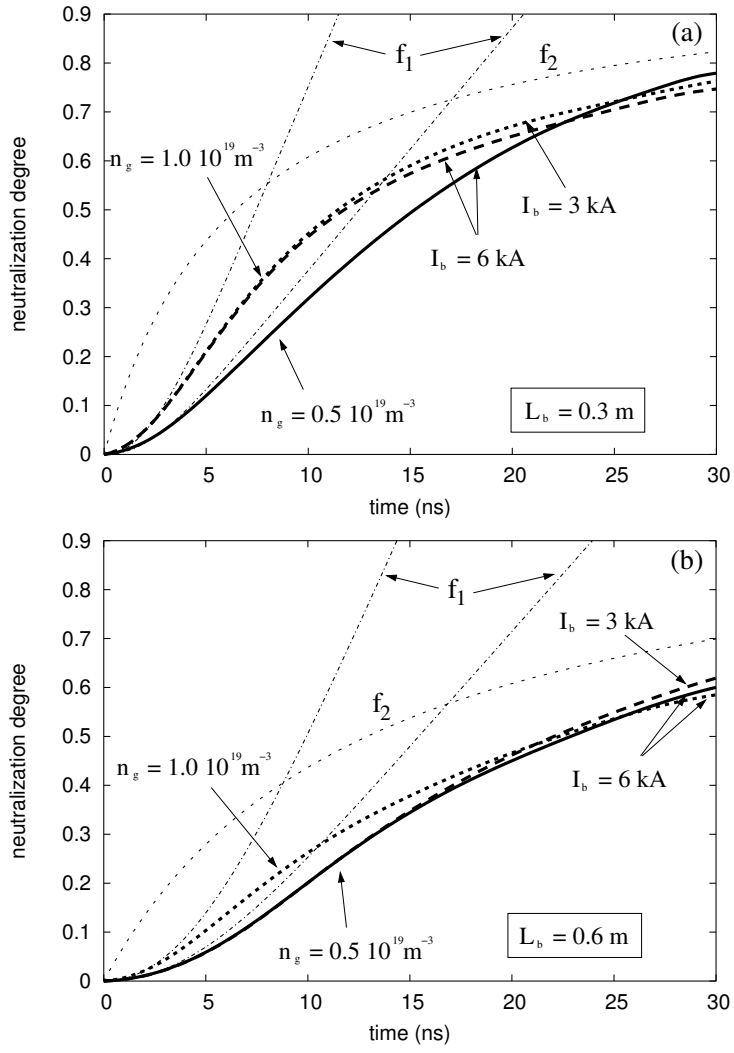


Fig. 5. Neutralization degree by ionization of background gas as a function of time for beams with frozen charge state. (a) $L_b = 0.3$ m and (b) $L_b = 0.6$ m.

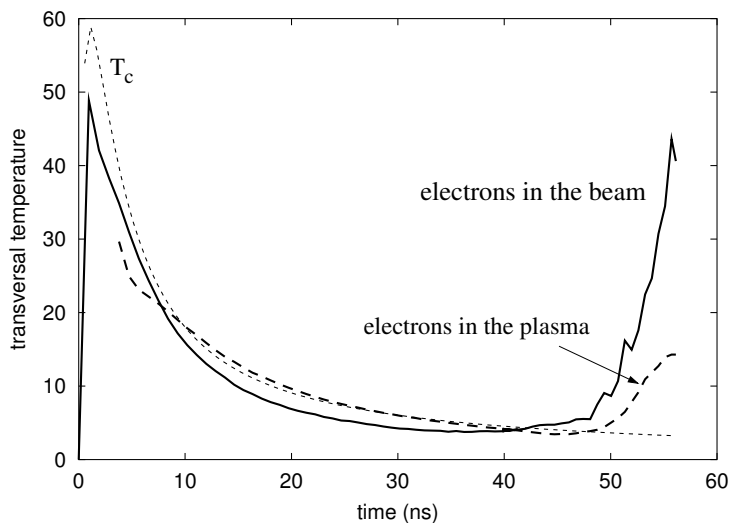


Fig. 6. Electron transversal temperature at the beam and at the plasma tail. T_c is the estimated temperature when compressional heating is neglected, given by equation 14. 2.5 GeV-Xe⁺ beam, $I_b = 3.8$ kA, $n_g = 5 \times 10^{19} \text{ m}^{-3}$, $L_b = 0.5$ m, $\hat{r}_{b0} = 0.05$ m, $L_f = 3$ m.